ELSEVIER

Journal of Hazardous Materials 74 (2000) 47–59

Journal of Hazardous Materials

www.elsevier.nl/locate/jhazmat

Partitioning behavior of trace elements during pilot-scale combustion of pulverized coal and coal–water slurry fuel

Irene G. Nodelman, Sarma V. Pisupati *, Sharon Falcone Miller, Alan W. Scaroni

Penn State University, Energy and Geo-Environmental Engineering Department and The Energy Institute, 110 Hosler Building, University Park, PA 16802, USA

Abstract

Release pathways for inorganic hazardous air pollutants (IHAPs) from a pilot-scale, down-fired combustor (DFC) when firing pulverized coal (PC) and coal–water slurry fuel (CWSF) were identified and quantified to demonstrate the effect of fuel form on IHAP partitioning, enrichment and emissions. The baghouse capturing efficiency for each element was calculated to determine the effectiveness of IHAP emission control. Most of the IHAPs were enriched in the fly ash and depleted in the bottom ash. Mercury was found to be enriched in the flue gas, and preferentially emitted in the vapor phase. When firing CWSF, more IHAPs were partitioned in the bottom ash than when firing PC. Significant reduction of Hg emissions during CWSF combustion was also observed.

Keywords: Partitioning; Combustion; Slurry fuel

1. Introduction

The 1990 Clean Air Act Amendments (CAAA) required the US Environmental Protection Agency (EPA) to assess the risk posed by fossil fuel power plant emissions and to establish appropriate regulations for their reduction. Combustion-derived inorganic hazardous air pollutant (IHAP) emissions are a consequence of energy production

* Corresponding author. Tel.: +1-814-865-0874; fax: +1-814-865-3248.
E-mail address: sxp17@psu.edu (S.V. Pisupati).

0304-3894/00/$ - see front matter
PII: S0304-3894(99)00198-3

and waste incineration. Although combustion processes are not the dominant sources of airborne IHAP emissions, they are among the significant contributors [9,16]. Some of the IHAPs may be partially removed by coal cleaning, trapped in the solid products (slag) of coal combustion, collected in fly ash, or escape to the environment in combustion gases. The major parameters that are vital to understanding IHAP behavior during combustion and prediction of the potential hazardous air pollutants (HAPs) emissions are the form in which a particular element occurs in coal, the element volatility, and its partitioning mechanism. Although there is a lack of information on trace element partitioning behavior during the burning of coal–water slurry mixtures, there are numerous studies of the fate, partitioning, and enrichment of trace elements during coal combustion. These studies have been carried out by Kaakinen et al. [4], Meij [7], Querol et al. [12], Ratafia-Brown [13], Swaine [17] and Tillman [18]. Partitioning refers to the dispersion of trace elements among different emission streams.

The focus of this study is eleven IHAPs: antimony (Sb), arsenic (As), beryllium (Be), cadmium (Cd), chromium (Cr), cobalt (Co), lead (Pb), manganese (Mn), mercury (Hg), nickel (Ni) and selenium (Se).

2. Objectives

The objectives of this study were to identify release pathways for trace elements from a pilot-scale combustion system while firing pulverized coal (PC) and coal–water slurry fuel (CWSF). The objectives also included an evaluation of the enrichment of trace element species in different emission streams. In this study, a Middle Kittanning seam coal was used in both pulverized form and as a CWSF.

3. Experimental

The experimental work was conducted in a pilot-scale down-fired combustion (DFC) test facility shown in Fig. 1. The combustor was designed for self-sustained combustion of various fuels (PC, CWSF and natural gas). The thermal input could be varied from 58.6 to 146.5 kW (200,000–500,000 Btu/h). Along with monitoring the data on gas and air flows, blower speed, flame signal and wall temperature profile, the flue gas composition (CO_2, CO, O_2, SO_2 and NO_x) was monitored using a Texas Micro Systems Data Acquisition System with ViewDac Software. The 3-m (9.84 ft) combustor has an internal diameter of 0.5 m and an outer diameter of 1.06 m. It is constructed in five modules. Each module consists of 0.457-m tall and 0.4-m diameter circular refractory sections. The combustor is lined with a 7.62-cm-thick Hydrecon 3000 refractory material to withstand temperatures up to 1650°C. A 0.2-m-thick, light weight, high alumina insulation layer was used to minimize heat loss and maintain a temperature of between 1450°C and 1500°C. The PC feed rate is controlled with an Accurate model 302 dry material feeder. The DFC generates 55–80 scfm of flue gas, which passes through a modular heat exchanger to lower the temperature to about 104°C (220°F) before entering the baghouse. The DFC is equipped with a pulse-jet baghouse (Ultra Model BB-9-58 III)

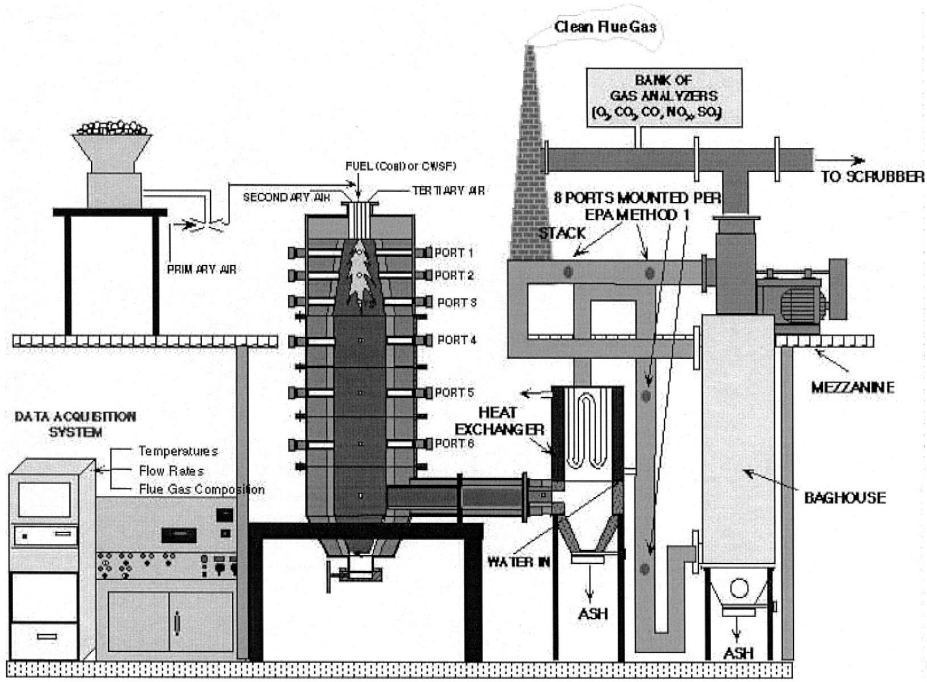

Fig. 1. Schematic diagram of the pilot-scale combustion test facility (not to scale).

with fiberglass felt bags with PTFE coating that fits over a mild steel cage. The baghouse has a filter area of 6 m^2 and an air to cloth ratio of 4.2:1 The bags provide a very high (up to 99%) collection efficiency for fine particles.

The combustion system is preheated by natural gas prior to firing PC or CWSF. The combustor was cleaned prior to each test to the extent possible by removing ash from the previous test run. The combustor was preheated using natural gas at a firing rate of 73.2 kW until the temperature reached approximately 1150°C. After the desired preheat temperature was reached, the PC was then admitted and its firing rate was gradually increased, while reducing simultaneously the natural gas rate until the desired load was obtained on coal. During testing, primary and secondary air flow rates, along with coal feed rates, temperatures, and emissions, were monitored at 1 min intervals to insure that the operating and test parameters were being maintained [11].

The quantification of trace elements in the pilot-scale combustor emission streams consisted of two principal steps: sample collection and laboratory analysis. To determine the pathways to the environment and to calculate the material balances for each trace element during each test run, the following streams were sampled and analyzed: (1) feed coal, (2) bottom ash, (3) heat exchanger ash, (4) baghouse inlet fly ash, (5) baghouse outlet fly ash and (6) baghouse ash.

Gaseous and particulate pollutants were withdrawn isokinetically from an emission source and were collected in a multicomponent sampling train. Isokinetic sampling is

defined as the uniform sampling of particles and gases moving within the stack. Isokinetic sampling is achieved when the gas velocity entering the sampling probe is the same as the gas velocity in the stack. This provides a uniform, representative sample of the particulate matter being emitted by the combustion source. The isokinetic sampling rate, or degree of isokineticity (% I), is defined as the ratio of the velocity of the sample gas inside the sampling probe to the average stack gas velocity.

3.1. Apparatus

Schematic representation of the Method 29 sampling train used in this study is shown in Fig. 2. This sampling train configuration is adapted from EPA Method 5 procedures, which, similar to multiple metals testing, are also applicable to particulate testing, acid gases testing and organics testing. The principal components of the sampling train are a heated fiberglass filter assembly and impingers loaded with hydrogen peroxide/nitric acid and potassium permanganate solutions. The other major parts of the sampling train are a buttonhook design nozzle, probe liner, a regular Pitot tube, impingers, and temperature and flue gas velocity metering systems. Construction details for the basic train components are given as part of EPA Method 5 [1,2]. According to Section 4 of EPA Method 2, the Pitot tube assembly coefficient was chosen to be 0.99 [1,2]. Quantities of crushed ice, ranging from 25 to 50 lb, were used during a sampling run, depending upon the ambient air temperature.

3.2. EPA Method 5 sampling train

Current EPA sampling and analysis methods for hazardous elements include Method 101A for mercury and Method 29 for multiple metals testing. Both methods are based on EPA Method 5 stack sampling probes and impinger trains. Method 101A uses potassium permanganate in sulfuric acid (4% $KMnO_4$/10% H_2SO_4) impingers to extract elemental mercury from a gas. Method 29 adds hydrogen peroxide–nitric acid (5% HNO_3/10% H_2O_2) impingers in front of the permanganate impingers to remove

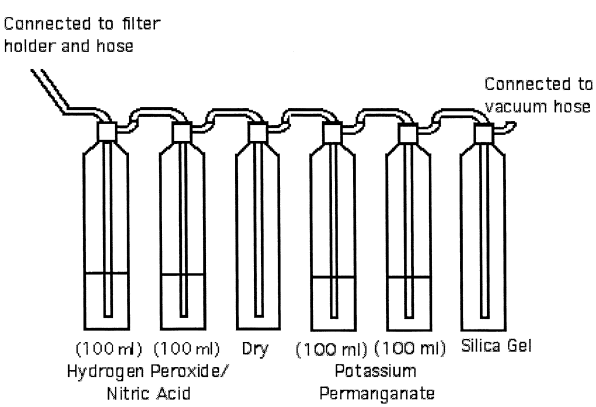

Fig. 2. Impinger assembly for Method 29 sampling train.

other metals. The sampling train also includes low metals background quartz-fiber filter, a Teflon™ frit, quartz nozzle, and probe.

The sampling trains were installed at the inlet and the outlet of the baghouse to determine the degree of penetration for each element through the baghouse. Particulate matter, including trace elements adsorbed on the surface, was collected in the probe and on the heated filter. Gaseous metals were collected in the back-half in chilled impingers containing aqueous solutions of dilute nitric acid combined with dilute hydrogen peroxide and dilute potassium permanganate.

3.3. Sample collection with Method 29 sampling train

During each test, the sampling probe was placed at four different horizontal traverse (sampling) points ($0.5 + 1.0 + 4.8 + 1.0$ in.[4] of the far stack wall) in order to provide a representative sample. The number and location of traverse points for all tests were determined according to EPA Method 1 for circular stacks and ducts, taking into consideration the internal diameter of the duct and the disturbance distance criteria. The sampling time at each point was 37.5 min (150 min total sampling time) to yield total sample volumes ranging from 0.8526 to 1.377 m^3 (30.11–48.64 ft^3). For each run, all required data, such as ambient, stack, probe, impinger, and meter temperatures, along with the sampled gas volumes and Pitot tube pressures were recorded. The difference between the initial and the final dry gas meter readings for each test was used to determine the volume of gas sampled (in ft^3).

Before each test run, the nozzle covering was removed and the nozzle was placed at the first traverse point with the tip pointing directly into the gas stream. At this point, it was verified that the Pitot tube and probe were properly positioned. When the probe was in the right position, the opening between the probe and stack access port was blocked off by coarse and fine adjustment valves to prevent unrepresentative dilution of the gas stream. Relocation of the sampling probe to the traverse point when sampling near the walls, and also removal or insertion of the probe through the access port were handled so as not to bump the probe nozzle into the stack walls. During the test run, the temperature at the fourth impinger's outlet was maintained near 20°C (68°F) by adding more ice around the impingers. At the end of the sample run, the adjusting valves were slowly opened, and the probe and nozzle were removed from the stack. The percent isokinecity was calculated after each run to determine whether the results were acceptable.

Following sampling, the disassembly of the train and sample recovery was performed.

3.4. Sample recovery

The first step in sample recovery was to disassemble the sampling train. The probe was cooled until it could be safely handled, and wiped off near the tip of the probe nozzle to remove all external particulate matter. The cap was placed over it to prevent loss or gain of particulate matter. Next, the sampling train was transferred to the clean-up area, where it was disassembled into the probe, the filter, and the impinger assembly. Teflon or glass caps were used to seal the liner outlet and filter inlet. The umbilical cord from the last impinger was removed and the impinger was cupped. The

sample lines from the filter and first impinger were also removed and cupped along with the filter and first impinger. Prior to and during disassembly, the train was inspected for any abnormal conditions. In order to recover all of the trace elements from the sampling train components, the impinger contents and rinses, along with the connecting elbows, filter, and probe rinses, were collected for digestion and analysis. The filter was carefully removed from the filter holder and placed in its identified petri dish. Any particulate matter and filter fibers, which adhered to the filter holder gasket, were also carefully transferred to the same petri dish.

Four samples were generated during each test: three liquid (probe rinse, combination of the first two impingers containing H_2O_2, and combination of the two $KMnO_4$ impinger solutions) and one solid (filter particulates).

3.5. Trace element analysis

Following the digestion in nitric and hydrofluoric acid, each sample was split for the analysis by graphite furnace atomic absorption spectroscopy (GF-AAS), cold-vapor AAS (CV-AAS), and direct current plasma emission spectroscopy (DCP-ES). The latter was used for the detection of Be, Co, Cr, Mn, and Ni. CV-AAS was used to analyze Hg. The remaining elements were detected by GF-AAS, using a Perkin-Elmer SIMAA 6000 spectrometer. The detection limits for Be, Co, Cr, Mn, and Ni were < 0.02 mg/g. The detection limit for Hg was 0.003 mg/g, and the detection limits for As, Se, Pb, Cd, and Sb were < 2.0, < 3.0, < 7.0, < 1.0, < 3.0 mg/g, respectively.

4. Results and discussion

The Middle Kittanning coal has an ash content of 5.19% and a sulfur content of 2.01% (Table 1). Trace element concentrations in the Middle Kittanning coal and CWSF are shown in Figs. 3 and 4, respectively. In order to estimate the IHAP partitioning behavior and calculate mass balances, all results were compared on the same basis

Table 1
Proximate analyses of test fuels and collected ash samples

	% Moisture[a]	% Volatile matter[b]	% Fixed carbon[b,c]	% Ash[b]
Middle Kittanning				
Coal	1.95	30.12	64.69	5.19
Bottom ash	1.49	8.85	42.35	48.80
Heat exchange ash	0.01	0.35	0.02	99.63
Baghouse ash	0.44	5.62	3.95	90.43
CWSF				
CWSF	38.39	30.77	64.08	5.15
Bottom ash	1.16	10.36	9.6	80.04
Heat exchange ash	0.64	13.06	3.29	83.65
Baghouse ash	0.91	7.46	4.98	87.56

[a] As received.
[b] Dry basis.
[c] Fixed carbon on a dry basis calculated by difference.

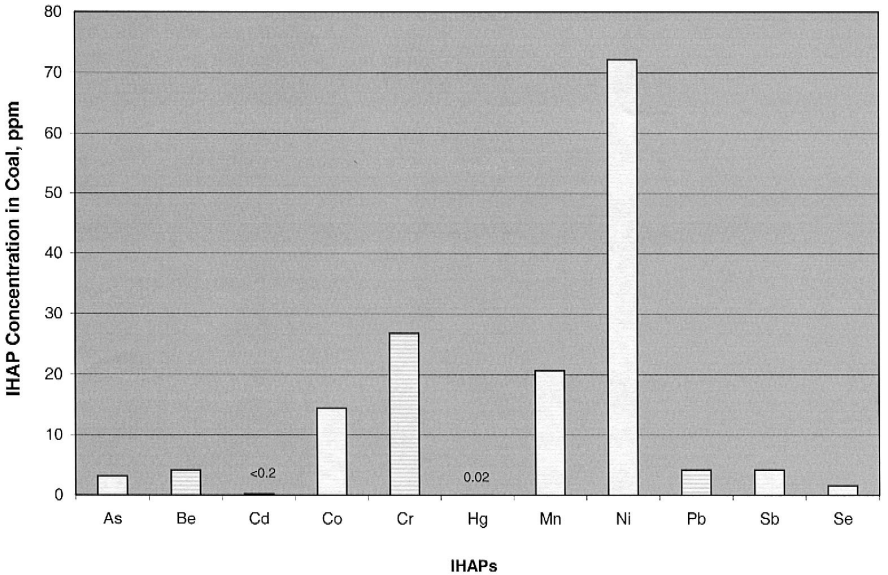

Fig. 3. IHAP concentrations in the Middle Kittaning PC (whole coal, parts per million basis).

(lb/10^{12} Btu) of heat input, which is commonly referred to as an ‘‘emission factor’’. The overall partitioning behavior of trace elements for the Middle Kittanning PC is shown in Fig. 5. A comparison of the trace element emission factors from the DFC and

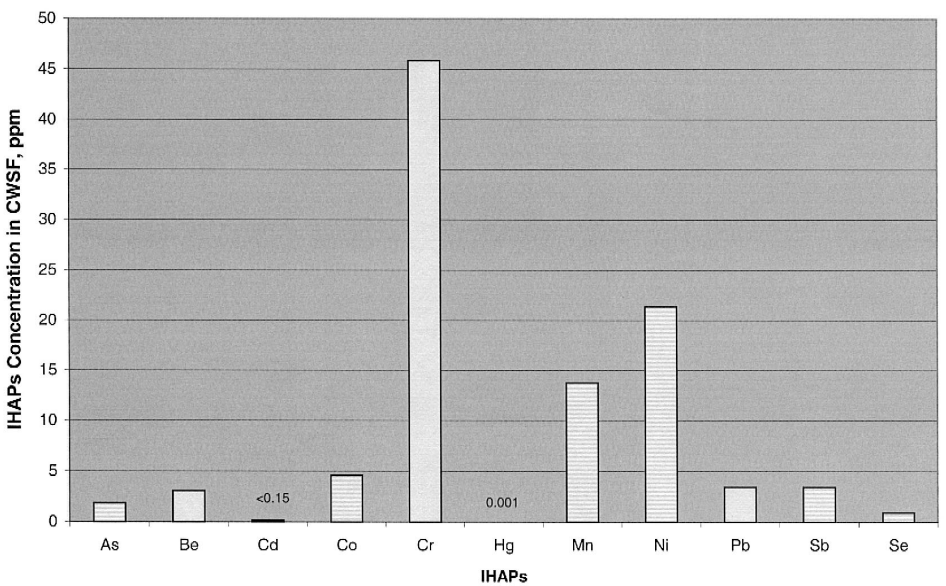

Fig. 4. IHAP concentrations in the Middle Kittaning CWSF.

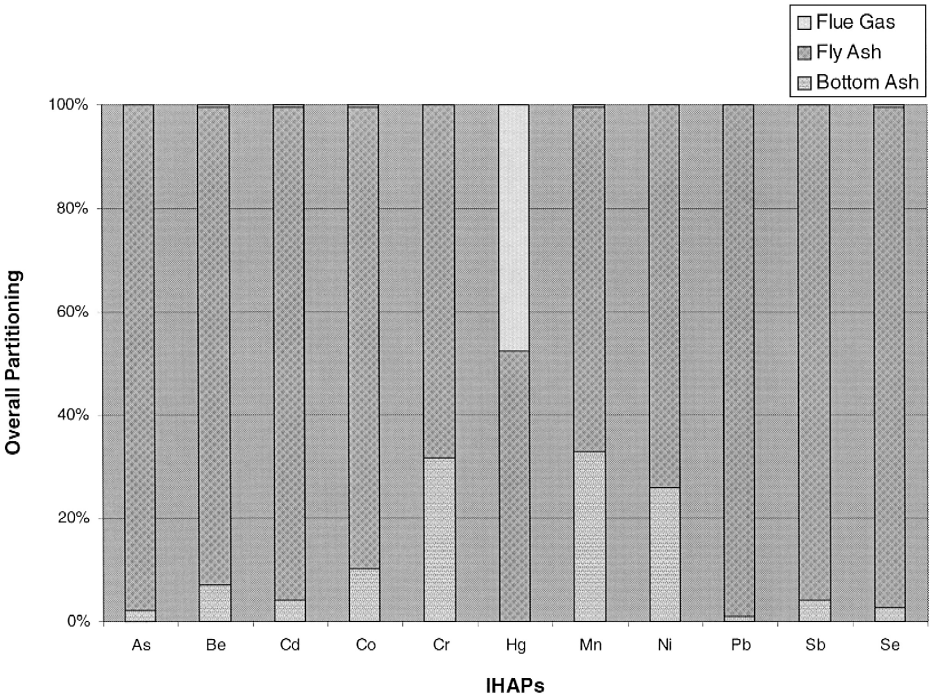

Fig. 5. Trace metal partitioning for the Middle Kittanning coal.

typical power plants is discussed elsewhere [14]. The CWSF, which was prepared from the Middle Kittanning coal, has a solids content of 61.3%. The overall trace elements' partitioning for the Middle Kittanning CWSF is presented in Fig. 6.

In general, most of the elements during the combustion of the CWSF were enriched in the fly ash emission stream. A method to compare the trace element concentration of one stream to that of another is by ''relative enrichment factor'' (REF). The REF concept was introduced by Meij [7], and is defined as:

$$\mathrm{REF} = \frac{(\text{Element Concentration})_{\text{ash}}}{(\text{Element Concentration})_{\text{coal}}} \times \frac{(\%\,\text{Ash content})_{\text{coal}}}{100}.$$

From Table 2, it can be seen that As, Be, Cd, Co, Hg, Pb, Sb, and Se have REF values ranging from 1.3 to 49, suggesting that portions of most of these elements were volatilized during combustion, and then, upon cooling, condensed on the fly ash particles, or partitioned between the fly ash particles and the gas phase. Cr, Mn, and Ni were enriched in the bottom ash, whereas Co showed no depletion or enrichment in the bottom ash emission stream. In general, the overall partitioning of IHAPs in the bottom ash emission stream is larger for CWSF than for PC. This is believed to be due to the differences in the temperatures and particle size distribution (PSD) of the char particles during the combustion. In a companion study firing micronized coal (MC) and micronized coal water mixture (MCWM) [10], it was observed that the gas temperature in

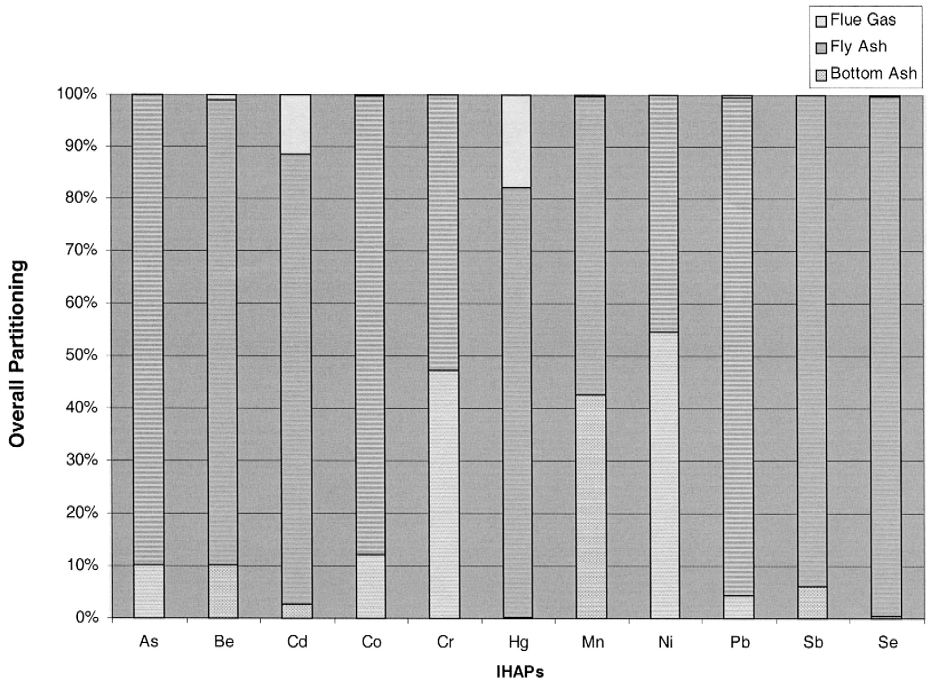

Fig. 6. Trace metal partitioning for the Middle Kittaning CWSF.

the case of MC firing, in a 454 kg/h (steam) water tube boiler, was higher than that in the MCWM test. This was partly due to the evaporation of water in the latter case. The average difference in the temperature measured across a vertical plane in front of the boiler for the MC and MCWM was about 442°C (337°F). The temperature difference remained about the same from the front (exit of the quartz) to the back of the boiler in the radiant section 429°C (313°F). Higher mean temperatures in front of the boiler indicate more rapid ignition and a higher rate of combustion, hence, higher heat release rates. Measurement of PSD indicated that there was a shift to larger top sizes when firing MCWM despite the similar PSD of the coal, fired as MC and MCWM. Coal particles are hydrophobic and tend to agglomerate in the presence of water molecules, which means that no matter how efficient the process of atomization, it is virtually impossible to produce droplets containing a single coal particle. Most of the atomization and combustion studies reported in the literature state that grinding the coal to ultra fine sizes to fire as CWSF will not provide the desired improvements in atomization and combustion [5,8]. Furthermore, since there is an additional step of evaporation of water involved in the sequential combustion process of MCWM, the overall time for combustion is longer, and therefore, for a given mean residence time, the char particles produced from MCWM tend to be larger. Large agglomerates burn inefficiently, requiring a long residence time for a complete burnout. Large agglomerates are unable to follow the gas flow and, therefore, contribute to the formation of ash deposits, or form slag deposits that can cause severe erosion of combustor surfaces [3]. In the case of

Table 2
Relative enrichment factors for tested species in all emission streams

	Bottom ash	Fly ash	Flue gases
Middle Kittaning			
As	0.61	3.51	0.03
Be	0.09	1.41	0.04
Cd	0.04	1.60	0.04
Co	0.12	1.31	0.05
Cr	0.63	4.51	0.02
Hg	0.01	7.18	20.46
Mn	0.22	1.23	0.03
Ni	0.19	1.55	0.01
Pb	0.02	1.91	0.01
Sb	0.01	1.45	0.01
Se	0.02	1.21	0.03
CWSF			
As	1.68	13.07	0.01
Be	0.43	2.31	0.06
Cd	0.03	1.30	0.07
Co	0.99	4.56	0.04
Cr	2.66	2.45	0.01
Hg	0.50	49.00	15.00
Mn	1.92	1.89	0.01
Ni	5.69	3.74	0.01
Pb	0.13	1.90	0.02
Sb	0.23	2.19	0.01
Se	0.05	5.71	0.03

Middle Kittanning PC, Hg was enriched in the flue gas emission stream; its overall partitioning in the flue gas was about 50%. As was mentioned above, when firing CWSF, Hg was enriched in the fly ash emission stream, and its overall partitioning in the flue gas emission stream was 20% less. This is a considerable reduction in Hg emissions. One can see that there was some partitioning of Cd (about 10%) in the flue gas emission stream. This ‘‘apparent’’ flue gas partitioning should be viewed with caution because the trace element analysis for Cd was under the detection limit for almost all emission streams (except fly ash at the inlet of the baghouse).

IHAP emissions at the baghouse outlet for Middle Kittanning PC and CWSF are presented in Fig. 7. Among the satisfactory mass balances obtained for IHAPs in the Middle Kittanning CWSF are Be (1.0), Mn (1.0), Cr (1.1) and Sb (0.9). The low mass balance for Cd (0.1) resulted from the very low (below detection limit) concentration of this element in the CWSF and almost all emission streams.

Removing volatile trace elements by coal cleaning prior to combustion is one option for trace element emission control. However, it is unlikely to provide complete removal of any trace element. Therefore, baghouse performance is very important for those elements that remain in the feed coal after cleaning. The majority of trace elements in most coals are contained within the fly ash. These elements tend to become enriched on the surface of fine-sized fly ash particles and escape particulate control devices. The

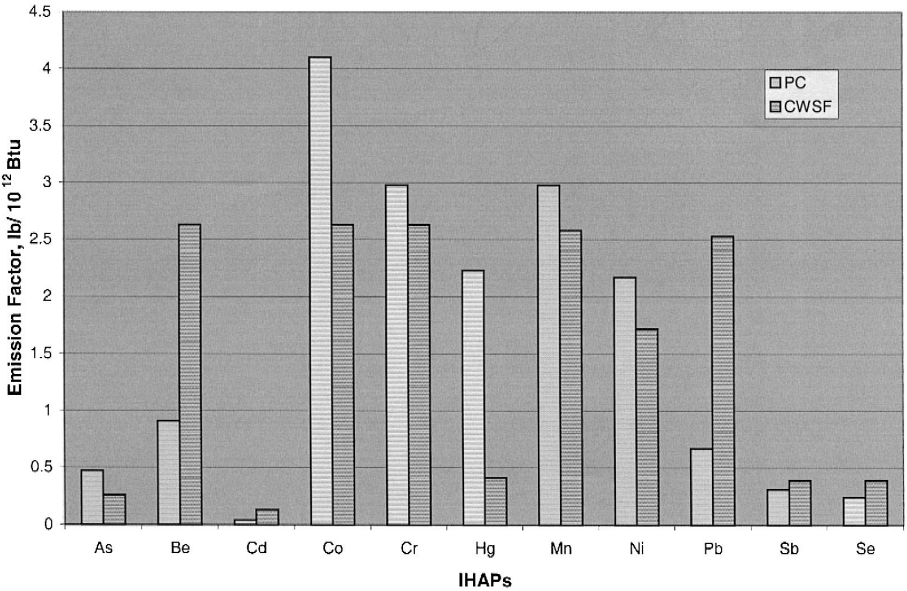

Fig. 7. Comparison between IHAP emissions at the outlet of the baghouse in Middle Kittaning PC and CWSF.

efficiency of the baghouse in these test runs for removal of air toxics for the Middle Kittanning PC and CWSF is presented in Table 3. The percent efficiency of capture for each element is calculated as follows:

$$\%\,\text{Efficiency} = \frac{(\text{Inlet flowrate} - \text{Outlet flowrate})}{\text{Inlet flowrate}} \times 100.$$

The results indicated that the baghouse efficiencies for As, Co, Cr, Mn, Ni, Pb, and Sb are 96–100%. It should be noted that particulate concentrations at the outlet of the

Table 3
Percent efficiency of baghouse

	Middle Kittanning PC	Middle Kittanning CWSF
As	100	100
Be	> 98	> 98
Cd	> 52	> 81
Co	> 93	99
Cr	> 93	100
Hg	29	73
Mn	> 87	> 98
Ni	> 98	100
Pb	99	> 99
Sb	> 98	100
Se	> 92	100

baghouse were reported as zero. This may not be wholly attributed to the efficiency of the baghouse. This is likely due to the low gas velocity in the duct at the sample point in the DFC. All of these elements, except Mn, belong to Class II elements (as defined by Meij [7]) and are enriched in the fly ash. Mn is classified as a Class I element and can be equally distributed between the bottom ash and the fly ash. This suggests that highly efficient baghouses (or other particulate control devices) would remove these elements quite well. This is in agreement with the results of this study that show the low concentrations of these elements in the stack. On the other hand, the test results for mercury emissions are in agreement with the previous literature data and suggest that most of these volatile elements remain in the flue gas beyond the baghouse. This element is almost fully emitted in the vapor phase and shows no enrichment in the fly ash. The baghouse removal efficiency for Hg is low: 29% for Middle Kittanning PC and 73% for CWSF. The baghouse ash from the Middle Kittanning PC and the CWSF test runs contained 9.57 and 12.44 wt.% combustibles, respectively. These vapor-phase Hg species are known to be captured by the unburned carbon in the ash. The residual carbon from coal combustion is believed to behave in the same manner as activated carbon, although the pore structure, surface properties, and inorganic content may be different. Combustibles in the fly ash were calculated by summing fixed carbon and volatile matter. Therefore, unburned carbon in the fly ash is assumed to be percent combustibles in the fly ash. The higher the combustible content in the fly ash for all test runs, the higher the baghouse capturing efficiency for Hg. Krishan et al. [6] and Senior and Morency [15] reported on the sorptive capacity of coal chars for oxidized mercury (HgO), mercury chloride ($HgCl_2$), and, to a lesser extent, elemental mercury (Hg^0) in the vapor phase.

5. Conclusions

The following conclusions were drawn regarding IHAP partitioning behavior with respect to different forms of fuel. The class II trace elements were enriched in the fly ash and depleted in the bottom ash as the result of initial vaporization and subsequent condensation on the submicron particulates. These elements were present in higher concentrations in the fly ash than in the bottom ash. In general, partitioning of some of IHAPs (e.g., Cr, Mn, Ni) in the bottom emission stream is greater for CWSF than for PC combustion due to lower temperatures associated with firing CWSF and possibly due to larger agglomerates produced from the coal–water droplets. Lower Hg emissions for CWSF combustion were observed. During the CWSF firing, Hg was enriched in the fly ash emission stream, and its overall partitioning in the flue gas emission stream was less than 20%. In comparison, during PC combustion, the overall partitioning of Hg in the flue gas was about 50%.

Acknowledgements

Financial support for this work was provided by the US Department of Defense and US Department of Energy under the cooperative agreement DE-FC22-92PC92162. The

assistance provided by the staff of the Energy Institute, particularly Ronald T. Wincek, is acknowledged.

References

[1] Code of Federal Regulations, Protection of Environment, Title 40, CFR, Part 61, Vol. 61, 1996, pp. 18260–18279.
[2] Code of Federal Regulations, Protection of Environment, Title 40, CFR, Part 60, 1996, pp. 562–579.
[3] R.L. Davidson, D.F.C. Natusch, J.R. Wallace, C.A. Evans, Trace elements in fly ash dependence of concentration on particle size, Environ. Sci. Technol. 8 (13) (1974) 1107–1113.
[4] J.W. Kaakinen, R.M. Jorden, M.H. Lawasani, R.E. West, Trace element behavior in coal-fired power plant, Environ. Sci. Technol. 9 (1975) 862–869.
[5] S.W. Kang, T.U. Yu, J.M. Beer, The significance of high shear viscosity for the atomization of CWF, in: Twelfth Annual ASME Energy Sources Technology Conference, American Society of Mechanical Engineers (ASME), 1988.
[6] S.V. Krishan, B.K. Gullett, W. Jozewicz, Sorption of elemental mercury by activated carbon, Environ. Sci. Technol. 28 (1994) 1506–1512.
[7] R. Meij, Trace element behavior in coal-fired power plants, Fuel Process. Technol. 39 (1994) 199–217.
[8] S.F. Miller, A comparison study of ash formation during pilot-scale combustion of pulverized coal and coal–water slurry fuels, PhD Thesis, The Pennsylvania State University, 1992.
[9] J.O. Nriagu, Natural versus antropogenic emissions of trace elements to the atmosphere,Fate and Control of Toxic Metals in the Atmosphere, Kluwer Academic Publishing, Dordrecht, 1989.
[10] S.V. Pisupati, R. Sharifi, Y. Liu, A.W. Scaroni, Measurements of temperature, particle size distribution and particle speed in an industrial boiler, in: Proceedings of the Thirteenth Annual Pittsburgh Coal Conference, Pittsburgh, PA, Sept. 3–6, 1996, University of Pittsburgh, Pittsburgh, 1996, pp. 1297–1302.
[11] S.V. Pisupati, G.A. Simons, K.H. Oehr, J. Zhou, Effect of BioLime™ atomization characteristics on simultaneous NO_x and SO_2 capture in coal combustion systems, in: Fourteenth Annual International Pittsburgh Coal Conference and Workshop, Taiwan, China, September 23–27, University of Pittsburgh, Pittsburgh, 1997.
[12] X. Querol, J.L. Fernandez-Turiel, A. Lopez-Soler, Trace elements in coal and their behavior during combustion in a large power station, Fuel 74 (1995) 331–343.
[13] J.A. Ratafia-Brown, Overview of trace element partitioning in flames and furnaces of utility coal-fired boilers, Fuel Process. Technol. 39 (1994) 139–157.
[14] A.W. Scaroni, B.G. Miller, S.V. Pisupati, International Research Center activities in coal combustion: Part 8. The energy institute, Prog. Energy Combust. Sci. 24 (1998) 450–456.
[15] C.L. Senior, J.R. Morency, Prediction of mercury speciation in coal-fired power plant flue gas: a fundamental study, in: Managing Hazardous Air Pollutants,Fourth International Conference, Washington, DC, November 12–14, 1997.
[16] I.M. Smith, Trace elements from coal combustion, Report No. IEACR/01, IEA Coal Research, London, 1987.
[17] D.J. Swaine, Trace elements and their dispersal during combustion, Fuel Process. Technol. 39 (1994) 121–137.
[18] D.A. Tillman, Trace Metals in Combustion Systems, Academic Press, San Diego, 1994.